

Effect of inter-wall surface roughness correlations on optical spectra of quantum well excitons

I. V. Ponomarev,* L. I. Deych, and A. A. Lisyansky

*Department of Physics,
Queens College of the City University of New York,
Flushing, NY 11367*

(Dated: November 20, 2018)

We show that the correlation between morphological fluctuations of two interfaces confining a quantum well strongly suppresses a contribution of interface disorder to inhomogeneous line width of excitons. We also demonstrate that only taking into account these correlations one can explain all the variety of experimental data on the dependence of the line width upon thickness of the quantum well.

PACS numbers: 71.35.Cc, 68.35.Ct, 78.67.De

I. INTRODUCTION

Absorption and luminescence exciton spectroscopy are one of the most important tools for studying quantum wells (QW) as well as other semiconductor heterostructures. Therefore, one of the most fundamental problems in physics of these systems is establishing connections between spectral line shapes and microscopic properties of the respective structures. A great deal of efforts was devoted to this problem over the last half of century, and it has been established, among other things, that at low temperatures the exciton line width in absorption and photoluminescence spectra in quantum wells is predominantly inhomogeneous¹. The shape of the spectra in this case is determined by various types of disorder present in a structure, and it is currently generally accepted that the spectral width in QW is directly related to the quality of interfaces, so that the luminescence spectra provide a quick and simple quality assurance tool for QW growth².

However, as it will be seen from the subsequent analysis, in spite of all the efforts, the existing theories of inhomogeneous broadening of excitons in QW still cannot satisfactorily explain all the diverse experimental data collected in this area. While it is quite plausible that the present theories suffer from several drawbacks, it is the goal of this paper to point out at one of the important circumstances completely overlooked in the previous studies. We will show here that it is not possible to explain experimental results collected by different groups for different material systems without taking into account so called *inter-wall correlations*, which describe the fact that properties of two interfaces forming a quantum well are correlated, especially for narrower wells. While direct morphological analysis done with cross-sectional scanning tunnel microscopy³, scattering ellipsometry⁴ and X-ray reflection measurements,^{5,6} give convincing experimental evidences of such correlations, their role in optical spectra of QW was never studied before. Another relevant example of such correlations is vertical stacking of quantum dots⁷, where vertical correlation length is observed up to the 80 monolayer thickness.

One of the main objectives of this paper is to show that the inter-wall correlations can significantly modify optical spectra, and that taking these correlations into account is necessary in order to achieve even a qualitative agreement between theory and experimental results. One of the important practical conclusions of this work is that narrow lines not always mean a good quality interfaces contrary to the popular belief, but can be the result of a line narrowing effect of the inter-wall correlations.

The paper is organized in the following way. In the next section we shall provide a brief review and critical analysis of existing experimental results and relevant theories. In subsequent section we will generalize the earlier theories of the interface disorder^{2,8,9,10,11} to include effects of the vertical correlations. In the last section we will compare the results of our analysis with experiments. The paper is concluded by an Appendix, in which we comment on the role of the lateral (in-plane) correlation length in the optical spectra of QW.

II. COMPARISON BETWEEN CURRENT THEORIES AND EXPERIMENT: CRITICAL REVIEW

Since a QW is generally a heterostructure formed by a binary semiconductor (AB) and a ternary disordered alloy ($AB_{1-x}C_x$), there are two types of disorder responsible for the inhomogeneous broadening. One is compositional disorder caused by concentration fluctuations in a ternary component of the QW as well as random diffusion across the interface^{12,13}. The other source of inhomogeneous broadening in QWs is associated with the roughness of the interface caused by the formation of monolayer islands at the interfaces resulting in local changes in the well thickness.^{2,8,9,10,11}

The quality of the interfaces is very sensitive to the ambient parameters of the growth process. Depending on growth conditions, the atoms deposited on the surface can form “islands” of various lateral sizes with different correlation scales. These morphological changes manifest themselves in the shape and width of optical spectra of QW excitons. Since both types of disorder can be ultimately traced to local changes in concentration, an accurate distinction between them is not a trivial task, and was first elucidated in Ref. 8.

Theoretical studies of effects due to compositional and interface disorder on absorption and photoluminescence spectra have a long history (for review articles see, for example, Refs. 1,14,15 and references therein.). This problem can be divided into two fairly independent parts. The first deals with the derivation of the random potentials acting on excitons in QW's from the properties of microscopic fluctuating parameters (concentrations, well thickness, etc.). Its main objective is to calculate correlation functions of these potentials. The second part of the problem consists of calculations of characteristics of excitons subjected to these potentials and in establishing relations between characteristics of optical spectra (line width, shape) and properties of the potentials (r.m.s. fluctuation and correlation length). Both these problems were carefully studied in the past, but since the focus of the present work is on the former we shall discuss it in more detail.

The main object of our discussion is the r.m.s value of the random potentials, W , defined as $W = \sqrt{\langle V_{eff}(\mathbf{R})^2 \rangle}$, and its dependence on the microscopic parameters of the QW. Here V_{eff} is the effective potential acting on excitons due to both compositional and interface disorder. Current theories predict distinctly different properties for contributions to the potential from these two types of disorder. In particular, the dependence of W upon the width of the well, L , for a narrow well is predicted as being $\propto L$ for the interface disorder. For the compositional disorder, it depends on whether the QW is formed by a ternary alloy or a binary system¹³. In the former case (as in $\text{In}_x\text{Ga}_{1-x}\text{As}/\text{GaAs}$) $W \propto L^{3/2}$, while in the case when the QW is formed by a binary material, the dependence is $W \propto \sqrt{L}$. In the three-dimensional limit $L \rightarrow \infty$ the contributions of the two types of disorder to $W(L)$ are also different. The contribution of the interface disorder for large L decreases as $1/L^3$, while the role of the alloy disorder again depends upon the type of the structure. If QW is formed by a ternary alloy W only weakly, as $1/\sqrt{L}$, decreases with the width before reaching a constant three dimensional limit. If, however, the alloy forms barriers, W decreases with L much faster as $\exp(-\kappa_0 L)/L^3$, where κ_0 is an inverse penetration length of ground state wave function in the barrier region. Although in both cases the function $W(L)$ has a maximum at some intermediate values of L , the position of the maximum, and the shape of the function $W(L)$ differ for the two types of disorder.

While the qualitative picture of disorder induced broadening is understood rather well, attempts at a quantitative comparison of theoretical predictions with experiments face significant difficulties. In Fig. 1 we have collected experimental data for dependencies of low temperature photoluminescence exciton line widths on QW average thickness, L . All the data are for $\text{In}_x\text{Ga}_{1-x}\text{As}/\text{GaAs}$ heterostructures, and represent experimental results from several research groups^{16,17,18,19}. While all the results show a non-monotonous dependence in accord with theoretical expectations, the maxima have different positions and, do not seem to have a regular dependence on concentration: the peak for $x = 0.18$ lies between peaks for $x = 0.12$ and $x = 0.135$. The maxima also have different heights and sharpness. For example, the full-width at half maximum (FWHM) for $x = 0.09$ and $x = 0.11$ have very smooth behaviors more characteristic for compositional disorder, while other data have rather sharp features more typical for interface disorder. Finally, the values of FWHM at large L , which are determined mainly by compositional disorder, are scattered over quite a broad range.

Let us analyze Fig. 1 in light of present theories. Regarding the alloy contribution to the line width, we note that in quantum mechanical approaches to this problem^{8,12,13,20} this contribution is completely determined by alloy concentration and QW width; the theories do not contain any unknown parameters that could be used to fit theoretical predictions to the experiments. Therefore, one can directly compare theoretical predictions with experimental results using the large L asymptote of the line width. Initial calculations for alloy induced disorder in the bulk^{12,21} and in the quantum wells¹³ were done in the adiabatic approximation, where Bohr's radius of an exciton, a_B , was assumed to be much larger than a correlation length of the effective potential, ℓ_c . If one applies that theory¹³ to the case of an $\text{In}_{0.12}\text{Ga}_{0.88}\text{As}/\text{GaAs}$ QW, the FWHM comes out to be = 0.36 meV for $L = 150 \text{ \AA}$. This value is much smaller than the observed bulk value³⁷. The same order of magnitude results are obtained in the semi-classical limit of the theory^{22,23} with the Gaussian shape of the exciton line width. One can reasonably argue¹ that the adiabatic approximation fails for a heavy hole and a light electron ($m_h \gg m_e$) both being subject to short-range energy fluctuations. Even for underlying “white-noise” disorder, the effective potential felt by an exciton has two different correlation lengths. A rather massive hole will average only the small volume around center-of-mass (COM) of the exciton, whereas a light electron is spread out over a much larger area of the order of a_B^2 . As a result, the hole will be much more sensitive to the compositional fluctuations, and its contribution to the effective disorder potential will be enhanced by the factor $(M/m_e)^2$, where $M = m_e + m_h$. However, the line widths found using improved theories^{8,20} turn out to be much larger than the experimental results (see also Fig. 7 below). Thus, existing theories cannot produce an accurate result for the alloy disorder contribution to the exciton line width.

It is less straightforward to compare the theory with experiments for interface roughness induced broadening because

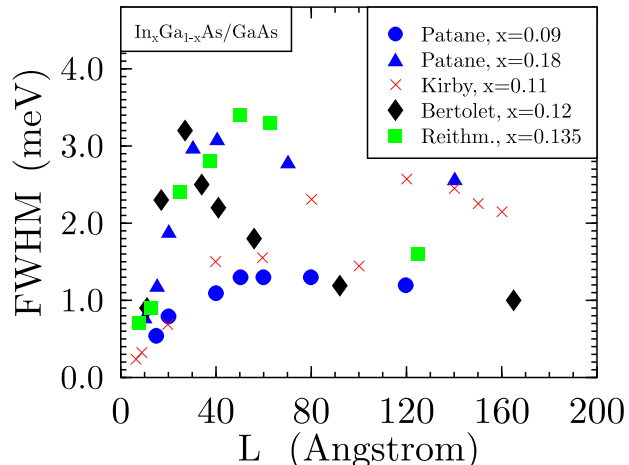


FIG. 1: Experimental dependences of the low temperature exciton full width on half maximum (FWHM) on the QW average size, L . All the data are presented for $\text{In}_x\text{Ga}_{1-x}\text{As}/\text{GaAs}$ QW's. The results were taken from the following references: Patanè, et al.¹⁶, Kirby, et al.¹⁷, Bertolet, et al.¹⁸, Reithmaier, et al.¹⁹.

it is difficult to separate contributions from two types of disorder in the regime of small and intermediate values of L . One could hope to identify the most important contribution by the slope of the $W(L)$ dependence at small L , but, unfortunately, the accuracy of the existing data does not allow one to distinguish between L or $L^{3/2}$ dependencies. The manifestation of the interface disorder in optical spectra is clearer in the case of systems where growth interruption resulted in formation of sufficiently large monolayer islands. It was shown in Ref. 11 that these islands could be responsible for the observed splitting of the exciton spectra. Also, interface roughness has been studied directly by such experimental techniques as microphotoluminescence, cathodoluminescence, transition electron microscopy, or scanning tunnelling microscopy.^{2,10,14,16,17,18,19,24,25,26,27}

The diversity of experimental behavior for FWHM shown in Fig. 1 presents a significant difficulty for existing theories of interface contribution to the line width^{8,28} even from the point of view of qualitative interpretation of the results. Indeed, the statistical properties of an interface are usually characterized by two length parameters: the thickness fluctuation, h , and the lateral (in-plane) correlation length, σ_{\perp} . With some reservations they are often taken to be equivalent to the average height and the lateral size of the islands at the interface. The size of height fluctuations, h , usually has a very restricted range of variations of one or two monolayers. In the semi-classical limit of the Gaussian shape line width, the broadening is proportional to the product $h\sigma_{\perp}$, which is really only one flexible parameter of the theory. With the help of this parameter it is possible to adjust the relative heights of the maxima but not their positions and particularly the sharpness of the peak. Even if one takes into account contributions from both types of disorder, it is still not possible to explain the variations between the optical spectra of different samples, a problem addressed in the last section of the paper.

It is clear from the provided analysis that existing theories of inhomogeneous broadening of excitons are unable to quantitatively explain experimental data. We suggest in this paper that one of the reason for this failure is the neglect of inter-wall correlations mentioned in the Introduction. While this idea does not fix the problems caused by wrong estimates of alloy disorder contribution, we will show in the subsequent sections of the paper that it does allow to explain all variety of experimental results related to the properties of the curves in Fig. 1 in the vicinity of their maxima.

III. STATISTICAL PROPERTIES OF THE INTERFACES AND EXCITON EFFECTIVE POTENTIAL

A. A model of the interface disorder

In order to make the problem tractable, we introduce standard simplifications assuming that both conduction and valence bands are non-degenerate, and that they both have an isotropic parabolic dispersion characterized by the masses m_e and m_h , respectively. Throughout the paper we use effective atomic units (a.u.), which means that all

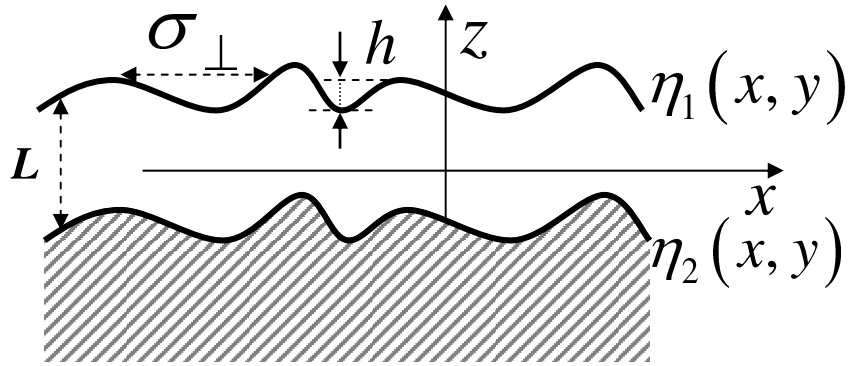


FIG. 2: Characteristic length scales describing interface roughness of a QW.

distances are measured in units of the effective Bohr radius $a_B = \hbar^2 \epsilon / \mu^* e^2$, energies in units of $E_{a.u.} = \mu^* e^4 / \hbar^2 \epsilon^2 \equiv 2 \text{ Ry}$, and masses in units of reduced electron-hole mass μ^* , where $1/\mu^* = 1/m_e^* + 1/m_h^*$. In this notation $m_{e,h} = m_{e,h}^* / \mu^*$, where $m_{e,h}^*$ are effective masses of an electron and a heavy hole. We will choose z -axes in the direction of growth of the structure (vertical direction). The plane perpendicular to this direction is the lateral plane (see Fig. 2). We measure electron and hole energies in the QW from the conduction and valence band edges of the barrier respectively. Then the potential of a QW with interface roughness is given by

$$U_{e,h}(\mathbf{r}) = -V_{e,h} [\theta(z + L/2 - \eta_1(x, y)) - \theta(z - L/2 - \eta_2(x, y))] \approx U_{e,h}^{(0)}(z) + \delta U_{e,h}^{intf}(\mathbf{r}), \quad (1)$$

where $\theta(z)$ is a step-function, $V_{e,h}$ are differences in off-set band energies, and

$$U_{e,h}^{(0)}(z) = -V_{e,h} [\theta(z + L/2) - \theta(z - L/2)], \quad (2)$$

$$\delta U_{e,h}^{intf}(\mathbf{r}) = V_{e,h} [\eta_1(x, y) \delta(z + L/2) - \eta_2(x, y) \delta(z - L/2)]. \quad (3)$$

Random functions $\eta_{1,2}(x, y)$, with zero mean, characterize the deviation of the i th interface from its average position. The perturbation expansion of the θ -function is justified because an interface roughness is almost always small for typical parameters in semiconductor heterostructures. The presence of two functions, $\eta_{1,2}(x, y)$, distinguishes Eq.(2) and Eq.(3) from the respective equations of Ref.8, where the roughness of only one interface was taken into account.

The statistical properties of the interfacial roughness in multilayered systems can be characterized by the height-height correlation functions

$$\langle \eta_i(\boldsymbol{\rho}_1) \eta_j(\boldsymbol{\rho}_2) \rangle = h^2 f_{ij} \zeta(|\boldsymbol{\rho}_1 - \boldsymbol{\rho}_2|), \quad (4)$$

where h is an average height of interface inhomogeneity, and $\langle \dots \rangle$ denotes an ensemble average. We assume here that the dependence of both diagonal and non-diagonal correlations on the lateral coordinates $\boldsymbol{\rho}$ is described by the same function $\zeta(\boldsymbol{\rho})$. For diagonal elements $f_{ii} \equiv 1$, and the respective functions describe lateral correlation properties of a given interface (*self-correlation functions*). Non-diagonal elements with $i \neq j$ introduce correlations between different interfaces; the respective quantity $f_{12}(L/\sigma_{\parallel})$, which can be called a *cross- or vertical-correlation function*, is a function of the average width of the well and is characterized by the vertical correlation length σ_{\parallel} (a subscript “ \parallel ” denotes that the direction of the vertical correlation is parallel to the direction of growth).

The effect of the inter-wall vertical correlations has been previously considered in studies of conductivity of thin metallic films^{29,30}. To the best of our knowledge, in all previous microscopic studies of the exciton line shape in optical spectra of QWs, these correlations were omitted. Such an approximation is valid for wide QWs, but in the case of narrow QWs the vertical correlations are experimentally confirmed^{3,4,5,6,7} and should be taken into account. In the limit $L/\sigma_{\parallel} \ll 1$ it is reasonable to assume that the inter-wall correlation function f_{12} tends to unity, which means that for the very small separation between the interfaces one random surface spatially repeats the pattern of the other. (See Fig. 2). As we shall see below, the effect of interface disorder in this case tends to cancel out at least in the first order of the perturbation theory. For the sake of concreteness we will assume below that

$$f_{12} = \exp(-L^2/\sigma_{\parallel}^2). \quad (5)$$

The value of the vertical correlation length σ_{\perp} depends on the growth process. In the following analysis we will also assume the Gaussian form for the lateral correlation function:

$$\zeta(\mathbf{R}) = \exp(-R^2/2\sigma_{\perp}^2). \quad (6)$$

The limit $\sigma_{\perp} \rightarrow 0$ corresponds to the “white-noise” correlator

$$\zeta(\mathbf{R}) = 2\pi\sigma_{\perp}^2 \delta(\mathbf{R}). \quad (7)$$

Following the standard procedure¹² described in numerous papers we derive the Schrödinger equation for the center of mass (COM) exciton motion subjected to an effective random potential,

$$\left[-\frac{\Delta_{\mathbf{R}}}{2M} + U_{eff}(\mathbf{R}) \right] \psi_i(\mathbf{R}) = \varepsilon_i \psi_i(\mathbf{R}), \quad (8)$$

with $U_{eff}(\mathbf{R})$ given by

$$U_{eff}(\mathbf{R}) = \int (\delta U_e + \delta U_h) \phi^2(\boldsymbol{\rho}) \chi_e^2(z_e) \chi_h^2(z_h) d^2 \rho dz_e dz_h \equiv U_e(\mathbf{R}) + U_h(\mathbf{R}). \quad (9)$$

where $\delta U_{e,h}$ are defined in Eq. (3), $\boldsymbol{\rho} = \boldsymbol{\rho}_e - \boldsymbol{\rho}_h$, and $\mathbf{R} = (m_e \boldsymbol{\rho}_e + m_h \boldsymbol{\rho}_h)/M$. For symmetric QW, $\chi(-L/2) = \chi(L/2)$, and from Eq. (3) we obtain

$$U_{e,h}(\mathbf{R}) = V_{e,h} \chi_{e,h}^2(L/2) \int [\eta_1(\mathbf{R} \pm \beta_{h,e} \boldsymbol{\rho}) - \eta_2(\mathbf{R} \pm \beta_{h,e} \boldsymbol{\rho})] \phi^2(\boldsymbol{\rho}) d^2 \rho. \quad (10)$$

Here $\beta_{h,e} = m_{h,e}/M$. Hereafter we will omit an explicit dependence on L for the electron and hole wave functions $\chi_{e,h}^2(L/2)$ always assuming that their values are taken at the position of the interface. The correlation function for the effective potential $U_{eff}(\mathbf{R})$ can then be expressed as

$$\langle U(\mathbf{R}_1) U(\mathbf{R}_2) \rangle \equiv T_{ee} + T_{hh} + 2T_{eh}, \quad (11)$$

where

$$T_{ii} = 2h^2 V_i^2 \chi_i^4 (1 - f_{12}(L)) \int d^2 \rho d^2 \rho' \phi^2(\rho) \phi^2(\rho') \zeta(|\mathbf{R} - \beta_j(\boldsymbol{\rho} - \boldsymbol{\rho}')|), \quad (12)$$

$$T_{eh} = 2h^2 V_e V_h \chi_e^2 \chi_h^2 (1 - f_{12}(L)) \int d^2 \rho d^2 \rho' \phi^2(\rho) \phi^2(\rho') \zeta(|\mathbf{R} - \beta_h \boldsymbol{\rho} + \beta_e \boldsymbol{\rho}'|), \quad (13)$$

where $i, j = e$ or h and $\mathbf{R} = \mathbf{R}_1 - \mathbf{R}_2$.

In all these expressions, the terms in front of the integrals determine the dependence of the correlation function on QW width L , while the integrals themselves determine the spacial correlations in lateral dimensions. Each of these terms can be presented in a form

$$T_{ij}(L, R) = 2h^2 V_i V_j F_{ij}(L) G_{ij}(R), \quad (14)$$

$$F_{ij}(L) = \chi_i^2 \chi_j^2 (1 - f_{12}(L)), \quad (15)$$

$$G_{ij}(R) = \int d^2 \rho d^2 \rho' \phi^2(\rho) \phi^2(\rho') \zeta(|\mathbf{R} - \beta_j \boldsymbol{\rho}' + \beta_i \boldsymbol{\rho}|), \quad (16)$$

where indexes i, j take values e and h (note that the order of these indices in the integrand is important).

B. Dependence on well thickness

Let us first focus on the functions $F_{ij}(L)$ which determine the dependence of the total correlation function on QW width L . For the sake of concreteness we consider in detail function F_{hh} . The analysis of other functions is similar. The dependence of F_{hh} on L comes from two factors. The first factor is the fourth degree of the electron QW wave function, χ_h^4 , calculated at the interfaces, $z = \pm L/2$. This dependence in In_{0.12}Ga_{0.88}As/GaAs QW is shown in Fig. 3 by a dashed line. It is easy to understand the behavior of χ_h^4 for the cases of large and small width. The characteristic scale here is given by $1/\kappa_{0h} = 1/\sqrt{2m_h V_h}$, since this scale determines the number of energy levels in a finite QW ($N = 1 + [\kappa_h L/\pi]$).

For finite QW the ground state wave function has a piece-wise form

$$\chi(z) = \begin{cases} A \cos(kz), & z \leq |L/2| \\ B \exp(-\kappa z), & z \geq |L/2| \end{cases} \quad (17)$$

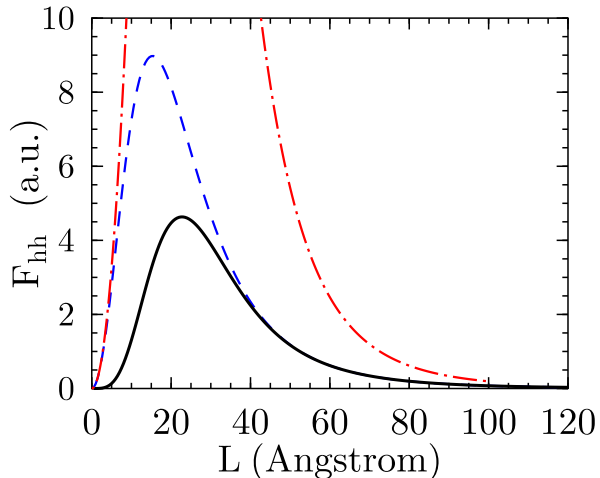


FIG. 3: Dependence of the correlation function of the hole-hole interface roughness potential on the well width in an $\text{In}_{0.12}\text{Ga}_{0.88}\text{As}/\text{GaAs}$ QW. The solid line is the function $F_{hh}(L)$. The dashed line is the fourth degree of the hole wave function at the interface. The dotted-dashed line shows approximations of this function for small and large L , given by Eqs. (19) and (20). The maximum of $\chi_h(L)^4$ is approximately located at $1/\kappa_{0h} = 1/\sqrt{2m_h V_h}$.

where $\kappa = \sqrt{\kappa_0^2 - k^2}$ and k is the ground state wave vector. From the normalization and matching conditions, one can readily obtain the value of square of the wave function at the interface

$$\chi^2 = B^2 \exp(-L) = \left[\frac{\kappa}{1 + \kappa^2/k^2 + \kappa L \kappa_0^2 / (2k^2)} \right]. \quad (18)$$

In the case of a wide QW, there are many discrete levels in the well, and the well is “almost infinite”: $k \approx \pi/L - 2\pi/L^2 \kappa_0$, $\kappa \approx \kappa_0$, and

$$\chi^2 \approx \frac{2\pi^2 \kappa_0}{\kappa_0^3 L^3 + 2\kappa_0^2 L^2 + 2\pi^2} \sim \frac{1}{L^3}. \quad (19)$$

Since for large well widths the vertical inter-wall correlations are negligible, $f_{12} \rightarrow 0$, Eq. (19) determines the total decrease of the interface correlator with increasing width.

In the opposite case of very narrow QWs, there is only one shallow level, which can be determined from the δ -functional potential approximation: $k \approx \kappa_0 - L^2 \kappa_0^3 / 8$, $\kappa \approx \kappa_0^2 L / 2$, and

$$\chi^2 \approx \frac{\kappa_0^2 L}{2}. \quad (20)$$

If one neglects vertical correlations, this expression describes the suppression of the interface disorder for narrow wells because of a decreased portion of the hole (electron) wave function inside the well. This result was obtained earlier in, for instance, Ref.22. Inter-wall correlations, however, significantly modify this dependence. For lengths smaller than the vertical correlation length σ_{\parallel} we have

$$1 - f_{12} \sim \left(\frac{L}{\sigma_{\parallel}} \right)^{\gamma}, \quad (21)$$

where γ is determined by the form of the inter-wall correlation factor f_{12} . For example, for Gaussian or Lorentzian dependences of $f_{12}(L)$, the parameter $\gamma = 2$, while for the exponential form of this function, $\gamma = 1$. Thus we obtain that, in narrow QWs, interface correlations are strongly suppressed by the factor

$$F_{ij}(L) \sim L^{2+\gamma}, \quad L < \sigma_{\parallel}, 1/\kappa_0. \quad (22)$$

While the transition between two asymptotic behaviors of χ is determined by the parameter κ_0 , the behavior of f_{12} depends on the correlation length σ_{\parallel} , which is a completely independent parameter. Experimental data suggest that

it is quite possible for σ_{\parallel} to be much larger than κ_0 . In this case, inter-wall correlations can affect not only the $L \rightarrow 0$ asymptotic of W , but also its behavior at $L \gg \kappa_0$. Instead of $1/L^3$ behavior one would have a much slower decrease of W with L : $W \propto L^{\gamma-3}$.

From the behavior of the wave function (18) we can see that the maximum of $F_{hh}(L)$ is reached in the vicinity of $L \sim 1/\kappa_{0h}$. However, as the previous analysis demonstrates, the vertical correlation function f_{12} can significantly shift this position; it can also change the height and shape of the peak. Thus, the presence of the inter-well correlation term $1 - f_{12}$ in function F_{hh} can naturally explain all variety of experimental results related to the properties of the curves in Fig. 1 in the vicinity of their maxima. The graph of function F_{hh} with inter-wall correlations taken into account is shown in Fig. 3. One can see that these correlations indeed significantly affect the shape of this function. While we only discussed properties of hole-hole correlator, it is clear that behavior of the electron-electron and hole-electron terms is similar.

C. Dependence on lateral correlation length

In order to investigate the results of the interplay between lateral and inter-wall correlations, let us now analyze the lateral correlation functions $G_{ij}(R)$. Their behavior is determined by the ratio of the potential correlation length, σ_{\perp} to the average size of the exciton in a plane, as well as by dimensionless parameters β_e and β_h . In order to evaluate the respective integrals, we chose the normalized ground state function of exciton relative motion in a quasi-two-dimensional form³¹

$$\phi(\rho) = \sqrt{\frac{2}{\pi\lambda^2}} \exp(-\rho/\lambda), \quad (23)$$

where λ is a variational parameter that indicates the average exciton size.

For the ground state function, Eq. (23), and the height-height correlation function, Eq. (6), the lateral dependence of the correlator $G_{ij}(R)$ can be presented as a function of two parameters $G_{ij}(R) \equiv G_{ij}(R; y_j, \alpha)$, where

$$y_i = \frac{\sqrt{2}\sigma_{\perp}}{\beta_i\lambda}, \quad (24)$$

and $\alpha = \min(\beta_i, \beta_j) / \max(\beta_i, \beta_j)$. Parameter α is equal to unity for the electron-electron and the hole-hole correlator. For the cross term G_{eh} this parameter is equal to m_e/m_h , which is much less than unity for the majority of semiconductor materials. This fact allows for additional simplifications when evaluating the integrals. The parameter $y_{e(h)}$ defines the ratio of the renormalized lateral correlation length $\beta_{e(h)}\lambda$ of the effective hole (electron) potential to the original correlation length of the interface fluctuations. For holes with $m_h \gg m_e$ this renormalized correlation length is much smaller than the corresponding length for the electrons. The latter implies that the interface disorder has a bigger impact on the holes compared to the electrons. This is also true for the contribution of alloy disorder to the broadening¹². Thus, the lateral correlation function can be rewritten in the following form:

$$G_{ij}(R; y_j, \alpha) = \frac{4y_j^4}{\alpha^2\pi^2} \int d^2\rho d^2\rho' \exp[-2y_j(\rho' + \alpha^{-1}\rho)] \exp(-|\mathbf{R} - \boldsymbol{\rho}' + \boldsymbol{\rho}|^2). \quad (25)$$

We shall focus on its value at the origin, $G_{ij}(0; y_j, \alpha)$, which determines the variance of the potential, W . The expression for W in this case can be presented in the following form:

$$W^2 = 2h^2 [1 - f_{12}(L/\sigma_{\perp})] [V_h^2 \chi_h^4 G_{hh}(0; y_e, 1) + 2V_e V_h \chi_e^2 \chi_h^2 G_{eh}(0; y_h, \alpha) + V_e^2 \chi_e^4 G_{ee}(0; y_h, 1)]. \quad (26)$$

The calculation are easier for the cross-term G_{eh} , because we can take advantage of smallness of $\alpha \ll 1$:

$$G_{eh}(0; y_h, \alpha) = 4y_h^2 \int dt t \exp(-t^2 - 2y_h t) + O(\alpha^2) = 2y_h^2 / (1 + \alpha)^2 - 2y_h^3 \exp(y_h^2) \sqrt{\pi} (1 - \text{erf}(y_h)) + O(\alpha^2), \quad (27)$$

where $\text{erf}(y)$ is the error function. The function (27) is shown in Fig. 4. It has the following behavior for small and large y :

$$G_{eh}(0; y_h, 0) \approx \begin{cases} \frac{4\sigma_{\perp}^2}{\lambda^2} - 2\sqrt{\pi}y_h^3 + \dots, & y_h \ll 1, \\ 1 - \frac{3}{2y_h^2}, & y_h \gg 1. \end{cases} \quad (28)$$

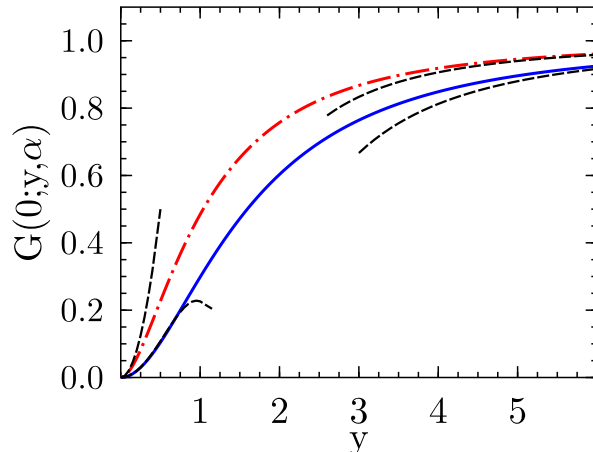


FIG. 4: Thick solid line is the lateral correlation function $G(0; y, 1)$. The dashed lines are its asymptotes given by Eq. (31). The thick dotted-dashed line is a cross-term correlator $G(0; y, 0)$. Its asymptotes (dashed lines) are given by Eq. (28)

The calculations are more cumbersome for the electron-electron and the hole-hole contributions $G_{ii}(0, y_j, 1)$. It is convenient to perform a transformation to the new set of coordinates which reflect the symmetry of the integral³²:

$$s = \rho_1 + \rho_2, \quad t = \rho_1 - \rho_2, \quad u = \rho_{12} = \sqrt{\rho_1^2 + \rho_2^2 - 2\rho_1\rho_2 \cos \theta}. \quad (29)$$

After this transformation³⁸ the calculations for G_{ii} are reduced to the one-dimensional integral

$$G_{ii}(0, y_j, 1) = y_j^4 \int_0^\infty ds e^{-2y_j s} \left[s + (2s^2 - 1) e^{-s^2} \frac{\sqrt{\pi} \operatorname{erf}(is)}{2i} \right]. \quad (30)$$

The term in square brackets in the integrand of Eq. (30) is a smooth function that behaves as $\sim (8/3)s^3$ for small s , and changes its behavior to $\sim 2s$ for $s > 1$. These dependencies allow one to estimate the asymptotic behavior for the correlator $G_{ii}(0; y_j, 1)$:

$$G_{ii}(0; y_j, 1) \approx \begin{cases} \frac{y_j^2}{2} - \frac{23y_j^4}{84}, & y_j \ll 1 \\ \frac{1}{1 - 3/y_j^2}, & y_j \gg 1. \end{cases} \quad (31)$$

The first terms in the series expansions of Eqs. (28) and (31) for small y correspond to the white-noise limit of the height-height correlation function, Eq. (7), and were obtained previously in Ref. 33. They can be readily derived by substitution of a δ -function instead of the last exponent in the integrand of Eq. (25). The consecutive terms in these formulas describe deviations from the white-noise model in the case of the short-range correlations. The dependence of correlators $G_{ij}(0; y, \alpha)$ on the respective parameters y_i is shown in Fig. 4, from which one can see that corrections to the white-noise approximation become significant even at relatively small values of the correlation length, σ_\perp .

For the “white-noise” interface roughness, Eq. (7), the analytical results can be obtained for the more elaborate exciton ground state trial function³⁴

$$\phi(\rho) = \frac{2 \exp(\gamma)}{\sqrt{2\pi\lambda^2(1+\gamma)}} \exp\left(-\sqrt{\rho^2/\lambda^2 + \gamma^2/4}\right), \quad (32)$$

which more accurately takes into consideration the three-dimensional character of the exciton. The parameter $\gamma = 2d/\lambda$ determines the ratio of the finite average distance d between the electron and the hole in the QW to the two-dimensional Bohr radius λ . In this case, one can obtain for the most important hole-hole correlator ($\alpha = 1$) the following expression

$$G(0, \sigma_\parallel, \{\lambda, \gamma\}, \beta, 1) = \frac{\sigma_\parallel^2}{\beta^2 \lambda^2} \frac{1 + 2\gamma}{(1 + \gamma)^2}. \quad (33)$$

This result formally coincides with the short-range limit $y^2/2$ of Eq. (31) after introduction of the renormalized effective Bohr radius $\tilde{\lambda} = \lambda(1+\gamma)/\sqrt{1+2\gamma}$. Since parameter γ in this expression is usually less than or of the order of unity, this renormalization is not significant, and we can conclude that an approximation of the exciton wave function by Eq. (23) gives reasonable results at least for the short-range interface disorder. Collecting together all results for the variance we obtain in the limit of short-range interface disorder

$$W^2 = 2h^2 [1 - f_{12}(L/\sigma_{\parallel})] \frac{\sigma_{\perp}^2}{\lambda^2} \left[\frac{V_h^2 \chi_h^4}{\beta_e^2} + 8V_e V_h \chi_e^2 \chi_h^2 + \frac{V_e^2 \chi_e^4}{\beta_h^2} \right]. \quad (34)$$

Apart from the vertical-correlation factor $1 - f_{12}$ this expression coincides with results obtained in Ref. 33. As expected, in the case when holes have a significantly larger mass than electrons (the typical situation for $\text{In}_x\text{Ga}_{1-x}\text{As}/\text{GaAs}$ or $\text{Al}_x\text{Ga}_{1-x}\text{As}/\text{GaAs}$ quantum wells), the hole-hole term in square brackets of Eq. (34) dominates. In the opposite limit of the long-range interface correlations the result is

$$W^2 = 2h^2 [1 - f_{12}(L/\sigma_{\parallel})] (V_h \chi_h^2 + V_e \chi_e^2)^2, \quad (35)$$

which agrees with the conclusion of Ref. 11 obtained for a different model of the interface disorder: in the regime of the long-range correlations the distribution of the effective potential reproduces the distribution of the interface roughness.

IV. COMPARISON WITH EXPERIMENTAL RESULTS

In order to compare calculations of W with experimental absorption spectra one needs to evaluate dynamics of excitons in a random potential with given correlation properties. This problem was intensively discussed in literature^{1,13,15,21} and we are going to use the results of the cited papers in conjunction with our analysis of the effective potential. There are two main models of exciton dynamics in a random model. One of them treats excitons quantum-mechanically in the limit of negative and large energies, while describing a most important intermediate region using an interpolation procedure^{13,21}. In this approach the absorption line has an asymmetric shape with the linewidth proportional to W^2 . In the second approach excitons are treated semiclassically¹; if the underlying compositional or interface roughness disorder is described by the Gaussian random process, then the shape of the exciton line is also approximately Gaussian with FWHM equal to $\Delta = 2\sqrt{2\ln(2)}W$. A transition between quasi-classical and quantum regimes of exciton dynamics is determined by a parameter $\nu = W/K_c$. Here $K_c = \hbar^2/2M\ell_c^2$ is a kinetic energy of an exciton confined in a spatial region of size ℓ_c , where ℓ_c is a suitably defined correlation length of the random potential¹⁵ (also see Appendix). The quantum limit corresponds to the case $\nu \lesssim 1$, while the semiclassical approximation is valid when $\nu \gg 1$.

In order to compare results obtained here with optical experimental data, we will make use of the semiclassical theory of exciton absorption, which according to Ref. 15 can be reliably applied to the situation under consideration (typical material parameters for an $\text{In}_x\text{Ga}_{1-x}\text{As}/\text{GaAs}$ QW yield $\nu \sim 5$ for $\sigma_{\perp} = 2a_{lat}$, and ν increases with increase of the correlation length). Using the semiclassical relation for Δ we plot the dependence of the interface roughness contribution to the exciton line width as a function of the well width in Figs. 5 and 6. Figure 5 represents curves for different lateral correlation lengths (“island sizes”), while Fig. 6 shows how these results are modified by the inter-wall correlations. The first thing to notice is that the changes in the lateral correlation length affect the height but not the position of the maximum and the shape of the curve. Comparison with the experimental data reproduced in this figure shows that an increase in σ_{\perp} drives the curves away from the experimental results. This has to be compared with the results of incorporating the inter-wall correlations, Fig. 6. An increase in σ_{\parallel} not only significantly reduces the height of the curve maximum, but also shifts its position toward larger values of L , and widens it.

It would be interesting to try to fit the experimental data presented in Fig. 1 with the results of our calculations. To this purpose one also needs to know the contribution of alloy disorder to the total line width. Making use of the model of short-range compositional disorder in a QW¹³ without the adiabatic approximation, one can obtain the following formula for the alloy disorder induced variance⁸:

$$\frac{a_{lat}^3 x(1-x)}{8\pi\lambda^2} \left[\frac{\alpha_h^2}{\beta_e^2} \int_{-L/2}^{L/2} \chi_h(z)^4 dz + 8\alpha_h\alpha_e \int_{-L/2}^{L/2} \chi_h(z)^2 \chi_e(z)^2 dz + \frac{\alpha_e^2}{\beta_h^2} \int_{-L/2}^{L/2} \chi_e(z)^4 dz \right], \quad (36)$$

where a_{lat} is the lattice constant, and $\alpha_{e,h} = dV_{e,h}/dx$ characterize the rate of the shift of conduction and valence bands with composition, x . The formula is given for the case of a QW made of a ternary alloy. The semiclassical theory of the exciton line width again yields: $\Delta = 2\sqrt{2\ln(2)}W$, while the interpolation procedure for the quantum limit

gives $\Delta \approx 0.59 MW^2$. The $\text{In}_{0.12}\text{Ga}_{0.88}\text{As}/\text{GaAs}$ QW is intermediate between these two limits, since $\nu \sim 1$. In Fig. 7 we present both Δ dependencies on well thickness. Unfortunately, as we can see, there exists a strong discrepancy between theoretical estimates of the contribution from alloy disorder and experimental results. It is not the goal of this paper to uncover the causes of this discrepancy. However, common wisdom tells us that in the bulk limit of very wide QW ($L > a_B$) only alloy disorder contribution should survive. The simplest way to adjust the theory is to introduce a phenomenological scaling down of Δ_{comp} to the value that should coincide with experimental results in the limit of large L asymptote. Although at present the reason for such re-scaling is unknown, it is hard to imagine that the proper theory of alloy disorder contribution will change the dependence of the variance on well thickness, L , determined by the integrals in Eq. (36). Since our main purpose is to elucidate the role of the inter-wall correlations rather than to revise existing theories of the alloy disorder, we carry out this operation keeping in mind its purely technical nature. The results of the best fit performed in this way are shown in Fig. 7 along with the best fit values of lateral and vertical correlation lengths. Performing a similar fitting procedure for other experimental dependencies of FWHM on well thickness shown in Fig. 1 we obtained the following values (normalized on lattice constant a_{lat}) for lateral and inter-wall correlation lengths in $\text{In}_x\text{Ga}_{1-x}\text{As}/\text{GaAs}$ QWs: for $x = 0.09$ $\sigma_{\perp} = 1$, $\sigma_{\parallel} = 20$, for $x = 0.18$ $\sigma_{\perp} = 1$, $\sigma_{\parallel} = 10$, for $x = 0.11$ $\sigma_{\perp} = 1$, $\sigma_{\parallel} = 5$, for $x = 0.12$ $\sigma_{\perp} = 1$, $\sigma_{\parallel} = 3$, for $x = 0.135$ $\sigma_{\perp} = 4$, $\sigma_{\parallel} = 13$. The most important result of this exercise is the demonstration that the fit would not be possible at all without taking into account the inter-wall correlations. We would also like to stress that it is not possible to achieve a good agreement with experimental results by omitting the inter-wall correlations, and using only alloy disorder scaling as an additional fitting parameter. We conclude, therefore, that the inter-wall correlations play an important role and must be taken into account when interpreting experimental results.

V. CONCLUSION

In conclusion, in this work we address the influence of vertical inter-wall correlations between rough interfaces on the exciton line shape. We show that the presence of these correlations strongly suppresses the interface disorder contribution into inhomogeneous broadening. The latter means that for narrow quantum wells it might happen that the exciton line width tells more about the quality of barrier material than about the quality of interface contrary to what is often claimed in the experimental literature. On the other hand, the differences in inter-wall correlation lengths can account for the variety of positions, strengths and sharpness of FWHM dependence on the well width for experimental data, obtained by different research groups.

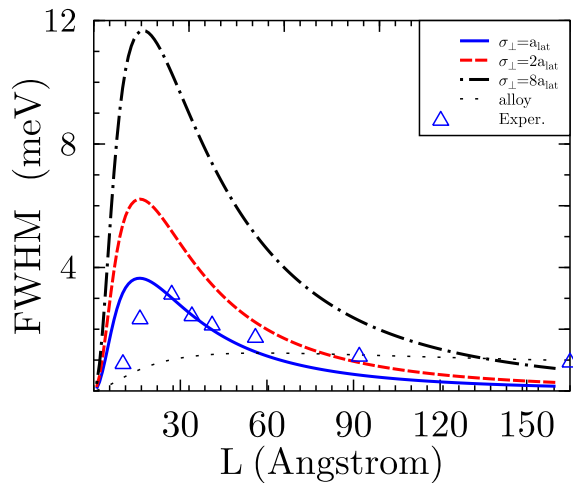


FIG. 5: Dependence of the interface roughness induced broadening on the perpendicular correlation length (“island size”) σ_{\perp} . The correlation length is given in terms of a number of lattice constants ($a_{lat} = 5.869\text{\AA}$). For all curves the composition concentration is $x = 0.12$, and the vertical correlation length parameter is fixed by $\sigma_{\parallel} = a_{lat}$. The dotted line is the rescaled alloy disorder contribution. The experimental data, shown by triangles, are taken from Ref. 18 and are presented here for comparison only.

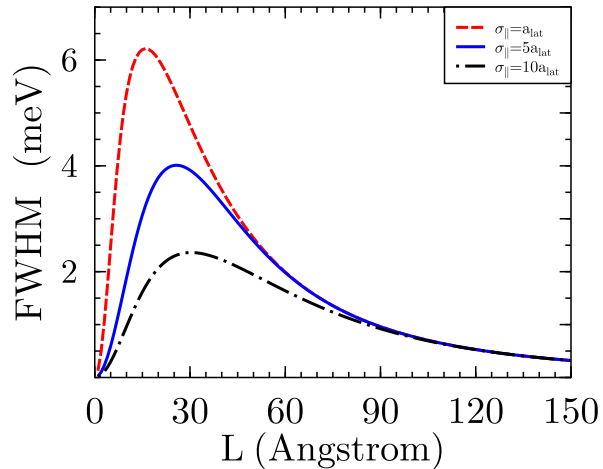


FIG. 6: Dependence of the interface broadening on the vertical correlation length (“island size”) σ_{\parallel} . All curves are drawn for $\sigma_{\perp} = 2a_{lat}$.

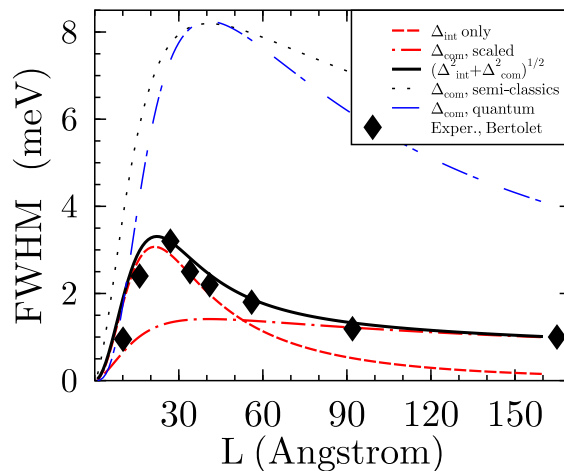


FIG. 7: The thick solid line is the best fit for the total line-width displayed together with experimental results (triangles) from Ref. 18. The separate contributions of the interface disorder (Δ_{int}) and of the rescaled alloy disorder (Δ_{alloy}) are also shown. The parameter-free theory for alloy disorder contribution discussed in Ref. 13 is shown by the dashed-dotted line (without adiabatic approximation). The semiclassical limit of the alloy disorder contribution⁸ is shown by the dotted line. The fitted parameters are $\sigma_{\parallel} = 3a_{lat}$, $\sigma_{\perp} = 1a_{lat}$.

Acknowledgments

We are grateful to S. Schwarz for reading and commenting on the manuscript. The work is supported by AFOSR grant F49620-02-1-0305 and PSC-CUNY Research grants.

APPENDIX A: DEPENDENCE OF THE LATERAL CORRELATION FUNCTION ON R

Calculation of the exciton absorption line shape is equivalent in the dipole approximation to the estimation of the optical density (OD) function¹:

$$A(\varepsilon) = \left\langle \sum_i \left| \int d^2 R \psi_i(\mathbf{R}) \right|^2 \delta(\varepsilon - \varepsilon_i) \right\rangle, \quad (\text{A1})$$

where ε_i and $\psi_i(R)$ are corresponding energy and wave function of the Schrödinger equation (8) for exciton COM. The shape of $A(\varepsilon)$ depends on the strength of disorder. The latter can be roughly measured by parameter $\nu = W/K_c$, where $W = \sqrt{\langle U_{eff}(R)^2 \rangle}$ is a variance of the potential energy induced by fluctuations and $K_c = \hbar^2/2M\ell_c^2$ is the kinetic ("correlational") energy of the exciton. The parameter ℓ_c determines the confinement of the exciton COM wave function. It can be extracted from knowledge¹⁵ of the lateral dependence on R for the correlation functions $G_{ij}(R, y_j, \alpha)$ since

$$\ell_c^D = \int d^D R' \langle U(\mathbf{R})U(\mathbf{R} - \mathbf{R}') \rangle / W^2. \quad (\text{A2})$$

For the "white-noise" height-height correlator (7) one can show that all distances are scaled by factors $(\lambda\beta_i)/2$, i.e. $\tilde{R} = 2R/(\lambda\beta_i)$. For the cross-term correlator in the limit of heavy holes and light electrons the result is simple again

$$G_{eh}(R; y_h, \alpha) \approx G_{eh}(R; y_h, 0) = 2y_h^2 \exp(-\tilde{R}), \quad (\text{A3})$$

while for the diagonal terms we have $G_{ii}(R; y_j, 0) = y_j^2/2f(\tilde{R}_i)$, where

$$f(\tilde{R}) = \frac{4}{\pi} \int_0^\pi d\theta \int_0^\infty d\rho \rho \exp\left(-\rho - \sqrt{\tilde{R}^2 - 2\rho\tilde{R}\cos\theta + \rho^2}\right). \quad (\text{A4})$$

Function $f(\tilde{R})$ has the following limits for small and large distances:

$$f(\tilde{R}) \approx \begin{cases} 1 - \frac{1}{4}\tilde{R}^2 + \frac{1}{12}\tilde{R}^3, & \tilde{R} < 1 \\ \sqrt{\frac{\pi\tilde{R}^3}{8}} \exp(-\tilde{R}), & \tilde{R} \gg 1. \end{cases} \quad (\text{A5})$$

Thus, even though the initial correlator of interface fluctuations was of the white noise type, the effective noise for the exciton potential is colored with exponential tails and with a correlation length of the order of the exciton radius. Similar results were obtained earlier for the bulk compositional fluctuations³⁵ and for the island model of interfacial roughness¹¹. One can show that such exponential asymptotes also persist for the long-range Gaussian correlator, Eq. (6), when $R/y \gg 1$. Since

$$G_{ee}(R) = \left(\frac{m_e}{m_h}\right)^2 G_{hh}\left(R\frac{m_e}{m_h}\right), \quad (\text{A6})$$

we can see that the lateral part of the electron-electron correlation function is suppressed by the factor $(m_e/m_h)^2$ but has larger correlation length. Overall, the localization length, ℓ_c , is determined however by the hole-hole term: $\ell_c \sim \lambda\beta_e$. The normalized lateral correlation functions $G_{ij}(R)$ are shown in Fig. 8.

* Electronic address: ilya@physics.qc.edu

¹ A. L. Efros and M. E. Raikh, in *Optical Properties of Mixed Crystals*, eds. R. J. Elliott and I. P. Ipatova, p. 133 (North-Holland, Amsterdam, 1988).

² C. Weisbuch, R. Dingle, A. Gossard, and W. Wiegmann, *Solid State Communications* **38**, 709 (1981).

³ Y. Yayon, A. Esser, M. Rappaport, V. Umansky, H. Shtrikman, and I. Bar-Joseph, *Phys. Rev. Lett.* **89**, 157402 (2002).

⁴ T. A. Germer, *Phys. Rev. Lett.* **85**, 349 (2000).

⁵ V. Holý and T. Baumbach, *Phys. Rev. B* **49**, 10668 (1994).

⁶ E. A. Kondrashkina *et al*, *Phys. Rev. B* **56**, 10469 (1997).

⁷ D. Bimberg, M. Grundmann, and N. Ledentsov, *Quantum Dot Heterostructures* (John Wiley & Sons, Chichester, 1999).

⁸ R. Zimmermann, F. Grosse, and E. Runge, *Pure & Appl. Chem.* **69**, 1179 (1997).

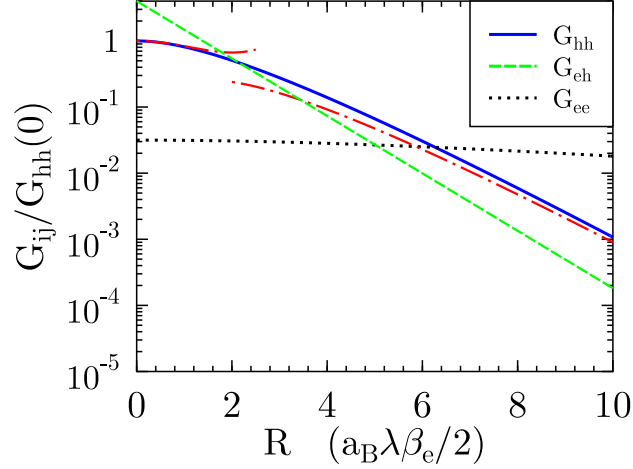


FIG. 8: Semi-log plot of the normalized lateral correlation functions $G_{ij}(R; y_j, \alpha)$. The normalization is chosen in a way to have the hole-hole correlator equal to unity at $R = 0$. Data are given for $y_h = 0.1$. The ratio $m_e/m_h = 0.178$ was chosen to depict the realistic case of InGaAs/GaAs QW. The dotted-dashed lines for hole-hole correlator are limits of small and large \tilde{R} [See Eq. (A5)]

- ⁹ R. Zimmermann, *Physica Status Solidi B* **173**, 129 (1992).
- ¹⁰ V. Srinivas, J. Hryniewicz, Y. J. Chen, and C. E. C. Wood, *Phys. Rev. B* **46**, 10193 (1992).
- ¹¹ H. Castella and J. W. Wilkins, *Phys. Rev. B* **58**, 16186 (1998).
- ¹² S. Baranovskii and A. Efros, *Sov. Phys. Semicond.* **12**, 1328 (1978).
- ¹³ A. Efros, C. Wetzel, and J. Worlock, *Physical Review B* **52**, 8384 (1995).
- ¹⁴ M. Herman, D. Bimberg, and J. Christen, *Journal of Applied Physics* **70**, R1 (1991).
- ¹⁵ E. Runge, in *Solid State Physics*, eds. H. Ehrenreich and F. Spaepen (Academic, San Diego, 2002).
- ¹⁶ A. Patanè, A. Polimeni, M. Capizzi, and F. Martelli, *Phys. Rev. B* **52**, 2784 (1995).
- ¹⁷ P. B. Kirby, J. A. Constable, and R. S. Smith, *Phys. Rev. B* **40**, 3031 (1989).
- ¹⁸ D. Bertolet, J.-K. Hsu, K. M. Lau, E. Koteles, and D. Owens, *Journal of Applied Physics* **64**, 6562 (1988).
- ¹⁹ J.-P. Reithmaier, R. Höger, and H. Riechert, *Phys. Rev. B* **43**, 4933 (1991).
- ²⁰ S. Lyo, *Phys. rev. B* **48**, 2152 (1993).
- ²¹ M. E. Raikh, N. N. Ablyazov, and A. L. Efros, *Sov. Phys. Solid State* **25**, 199 (1983).
- ²² J. Singh and K. K. Bajaj, *J. Appl. Phys.* **57**, 5433 (1985).
- ²³ R. Zimmermann, *Journal of Crystal Growth* **101**, 346 (1990).
- ²⁴ H. Zhao, S. Moehl, and H. Kalt, *Physical Review Letters* **89**, 097401 (2002).
- ²⁵ D. Bimberg, D. Mars, J. Miller, R. Bauer, and D. Oertel, *Journal of Vacuum Science & Technology B* **4**, 1014 (1986).
- ²⁶ A. Ourmazd, D. Taylor, J. Cunningham, and C. Tu, *Physical Review Letters* **62**, 933 (1989).
- ²⁷ J. Christen, M. Grundmann, and D. Bimberg, *Applied Surface Science*, **41-42**, 329 (1989).
- ²⁸ J. Singh, K. K. Bajaj, and S. Chaudhri, *Appl. Phys. Lett* **49**, 805 (1984).
- ²⁹ A. E. Meyerovich and A. Stepaniants, *Phys. Rev. B* **60**, 9129 (1999).
- ³⁰ A. Meyerovich and I. V. Ponomarev, *Phys. Rev. B* **65**, 155413 (2002).
- ³¹ G. Bastard, E. E. Mendez, L. L. Chang, and L. Esaki, *Phys. Rev. B* **26**, 1974 (1982).
- ³² H. A. Bethe and E. E. Salpeter, *Quantum mechanics of one and two electron systems* (Springer, Berlin, 1957).
- ³³ R. Zimmermann, *Japanese Journal of Applied Physics, Supplement* **34**, 228 (1994).
- ³⁴ I. V. Ponomarev, L. I. Deych, and A. A. Lisyansky, *Unpublished, cond-mat/0305405*.
- ³⁵ Z. S. Gevorkyan and Y. E. Lozovik, *Sov. Phys. Solid State* **27**, 1079 (1985).
- ³⁶ I. V. Ponomarev, V. V. Flambaum, and A. L. Efros, *Phys. Rev. B* **60**, 5485 (1999).
- ³⁷ In fact, the value calculated with the help of Eq. (A4) in Ref. 13 would be even smaller, since the authors omitted without any reasons the cross-term $2\alpha_e\alpha_h \int \chi_e^2 \chi_h^2 dz$ which is of the same order of value as other two terms.
- ³⁸ For detailed derivation of the volume element in two-dimensional case see Appendix B in Ref. 36